

Supporting Information

Comparison of microflow and analytical flow liquid chromatography coupled to mass spectrometry global metabolomics methods using a urea cycle disorders mouse model

Sarah Geller^{1,2}, Harvey Lieberman^{1†}, Adam J. Belanger^{1††}, Nelson S. Yew¹, Alla Kloss¹, Alexander R. Ivanov^{2*}

¹Sanofi, Waltham, MA, 02451, USA

²Barnett Institute of Chemical and Biological Analysis, Department of Chemistry and Chemical Biology, Northeastern University, Boston, MA, 02115, USA

†Current address: Novartis, Cambridge, MA 02139 USA

††Current address: Pfizer, Cambridge, MA 02139 USA

*Corresponding Author

Tel: +1 617 373 6549

E-mail: a.ivanov@northeastern.edu

Table of Contents

Figure S1. PCA plots of mouse brain homogenate samples

Figure S2. Representative results confirming the instrumental stability for the brain homogenate sample analysis in the positive ionization mode

Figure S3. Representative results confirming the instrumental stability for the brain homogenate sample analysis in the negative ionization mode

Figure S4. Representative Venn Diagram of those features with a %CV less than 75% for each sample group

Figure S5. Representative trend plots showing the desired trends for trend analysis filtering

Figure S6. Graphs of all identified metabolites present in mouse brain homogenate samples

Figure S7. PCA plots of mouse urine samples

Figure S8. Representative results confirming the instrumental stability for the urine sample analysis in the positive ionization mode

Figure S9. Representative results confirming the instrumental stability for the urine sample analysis in the negative ionization mode

Figure S10. Graphs of all identified metabolites present in mouse urine samples analyzed using the ion-pairing method in the positive ionization mode

Figure S11. Graphs of all identified metabolites present in mouse urine samples analyzed using the microflow method in the positive ionization mode

Figure S12. Graphs of all identified metabolites present in mouse urine samples analyzed using the ion-pairing method in the negative ionization mode

Figure S13. Graphs of all identified metabolites present in mouse urine samples analyzed using the microflow method in the negative ionization mode

Figure S14. Metabolic pathway map highlighting known UCD biomarkers

Table S1. Percentage of detected features calculated to be linear as grouped by retention time during dilution factor optimization

Table S2. Percentage of detected features calculated to be linear as grouped by m/z during dilution factor optimization

Table S3. Sample number per group for mouse brain homogenate samples analyzed using both ion-pairing and microflow based methods

Table S4. Sample number per group for mouse urine samples analyzed using both ion-pairing and microflow based methods

Table S5. Summary of the metabolites identified in the brain homogenate samples analyzed using the ion-pairing and microflow based methods

Table S6. Data processing step where metabolites were filtered out of for mouse brain homogenate samples in the positive ionization mode

Table S7. Data processing step where metabolites were filtered out of for mouse brain homogenate samples in the negative ionization mode

Table S8. Summary of the metabolites identified in the urine samples analyzed using the ion-pairing and microflow based methods

Table S9. Data processing step where metabolites were filtered out of for mouse urine samples in the positive ionization mode

Table S10. Data processing step where metabolites were filtered out of for mouse urine samples in the negative ionization mode

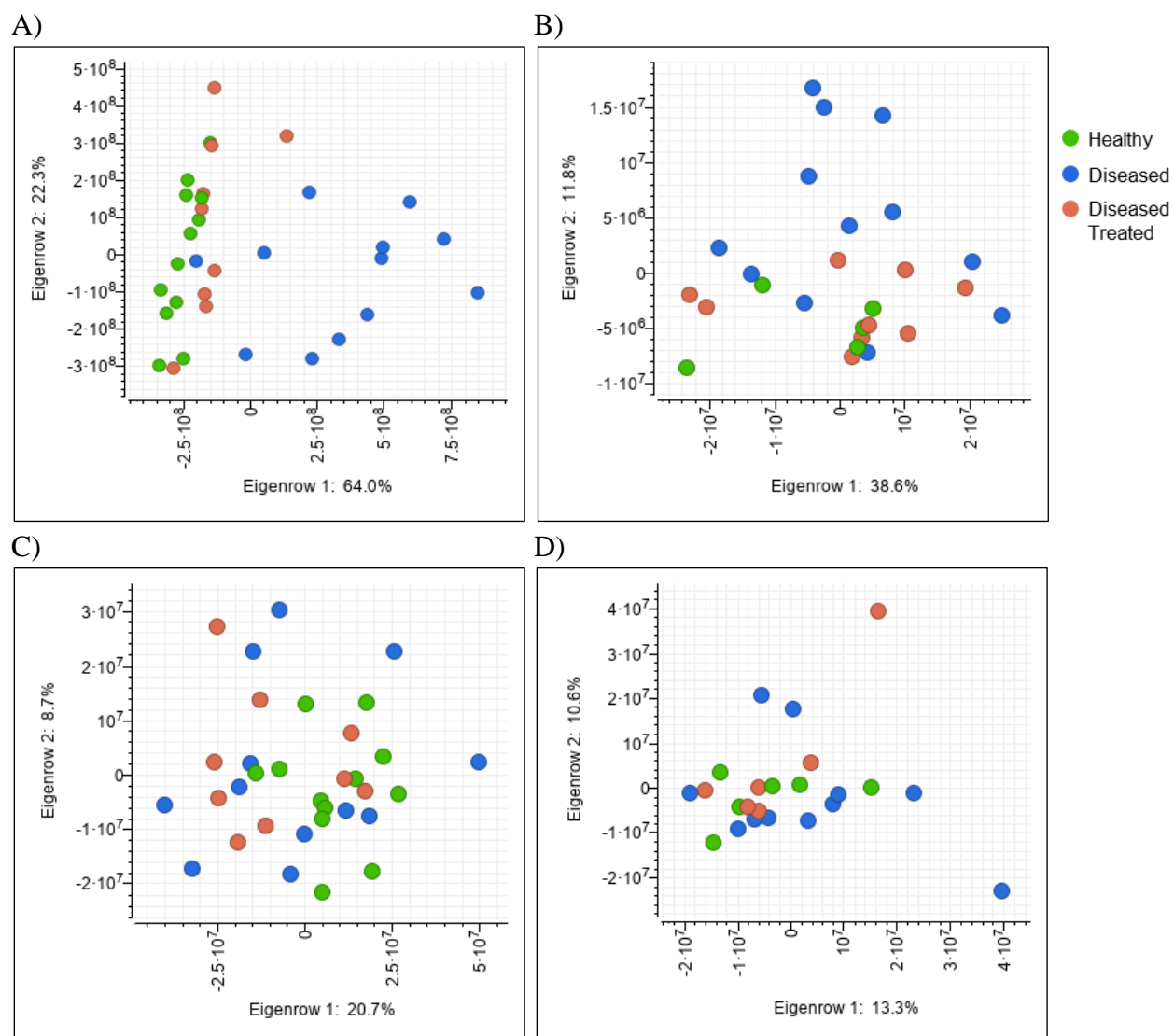


Figure S1. PCA plots of mouse brain homogenate samples. Shown are results from the positive ESI mode analysis using the A) ion-pairing-based LC method and B) microflow-based LC method; and the negative ESI mode analysis using the C) ion-pairing-based LC method and D) microflow-based LC method

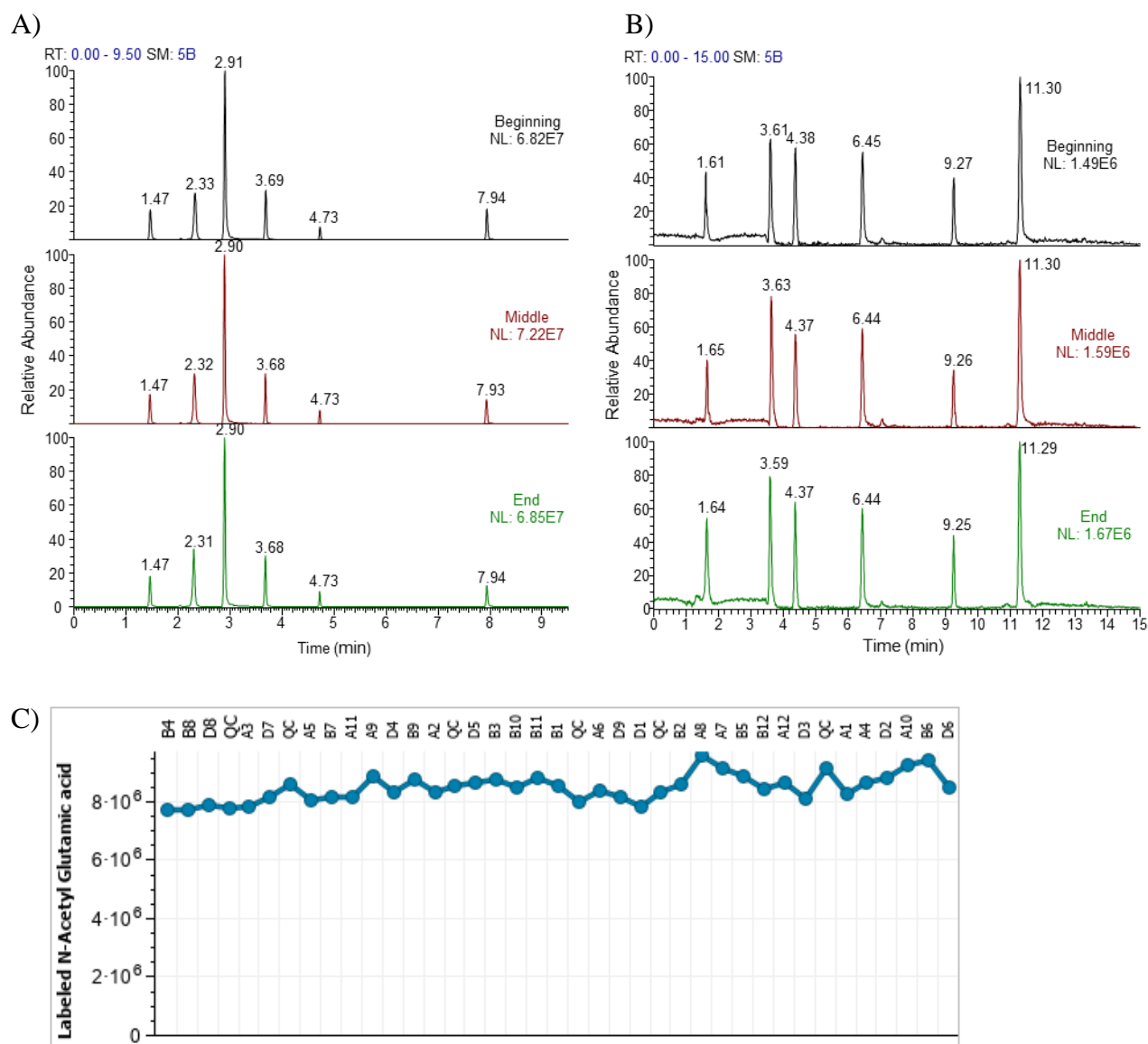


Figure S2. Representative results confirming the instrumental stability for the analysis of the brain homogenate samples analyzed using the microflow and analytical flow ion-pairing based methods in the positive ionization mode. A) Extracted ion chromatograms (5 ppm mass accuracy) of QC injections analyzed at the beginning, middle, and end of the ion-pairing method sequence. Analytes shown (from left to right): glycine, homoserine : threonine, nicotinamide, acetylcarnitine, tryptophan, sphinganine. B) Extracted ion chromatograms (5 ppm mass accuracy) of QC injections analyzed at the beginning, middle, and end of the reversed-phase microflow method sequence. Analytes shown (from left to right): deoxycarnitine, guanosine, tryptophan, azelate, hydroxyphenyllactate, sphinganine. C) The normalized maximum intensity of the isotopically labeled N-acetyl glutamic acid internal standard in all sample and QC injections analyzed using the ion-pairing-based method. The percent relative standard deviation of the internal standards across all sample and QC injections was < 20% with both methods.

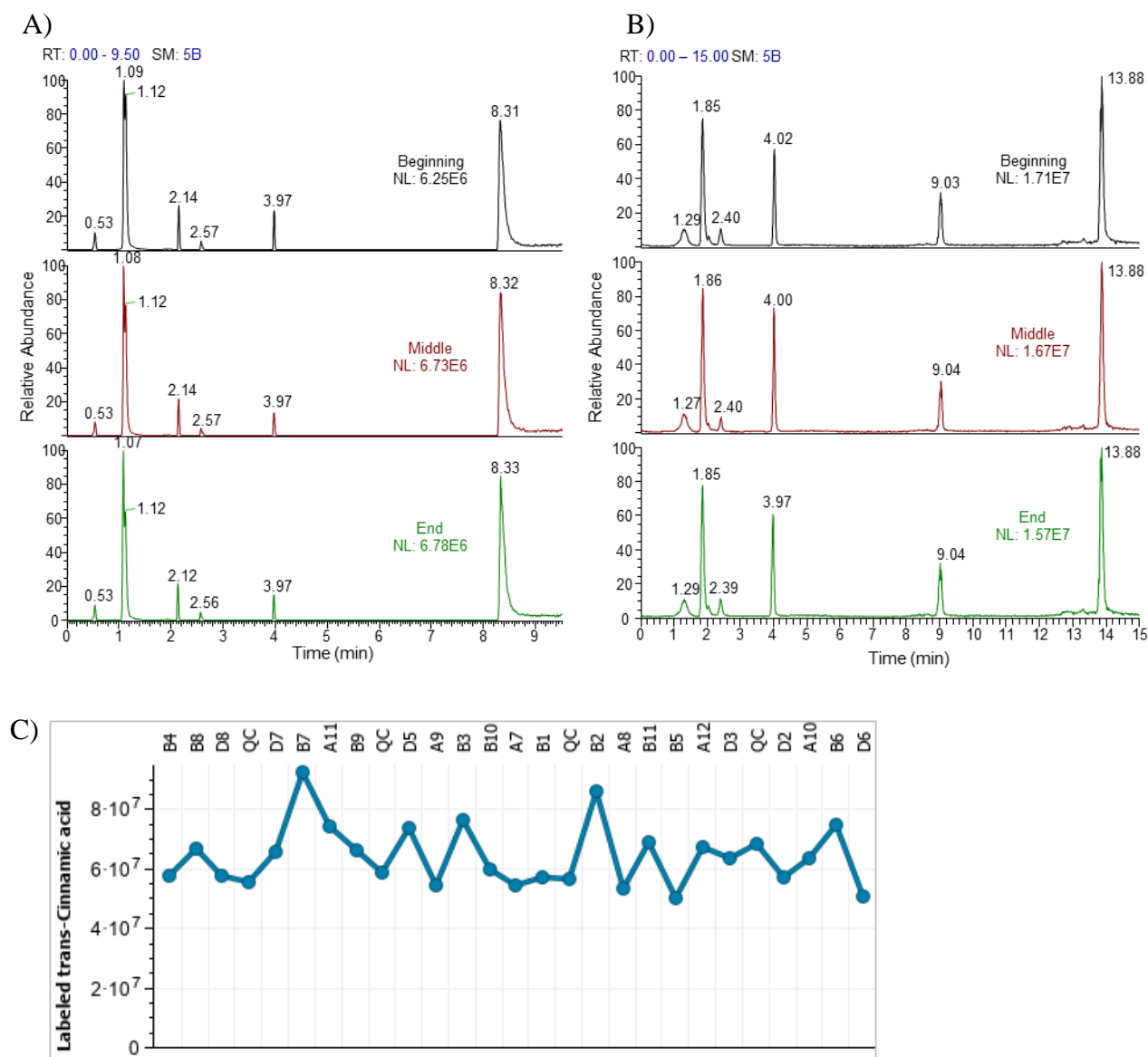


Figure S3. Representative results confirming the instrumental stability for the analysis of the brain homogenate samples analyzed using the microflow and analytical flow ion-pairing based methods in the negative ionization mode. A) Extracted ion chromatograms (5 ppm mass accuracy) of QC injections analyzed at the beginning, middle, and end of the ion-pairing method sequence. Analytes shown (from left to right): alanine : sarcosine, aspartic acid, inosine, glycerol 2-phosphate : sn-glycerol 3-phosphate, 2-phosphoglyceric acid, palmitic acid. B) Extracted ion chromatograms (5 ppm mass accuracy) of QC injections analyzed at the beginning, middle, and end of the reversed-phase microflow method sequence. Analytes shown (from left to right): glucose : other simple sugars, glutamic acid : N-acetylserine, glutathione, inosine, heptanoate, laurate. C) The normalized maximum intensity of the isotopically labeled trans-cinnamic acid internal standard in all sample and QC injections analyzed using the microflow method. The percent relative standard deviation of the internal standards across all sample and QC injections was < 20% with both methods.

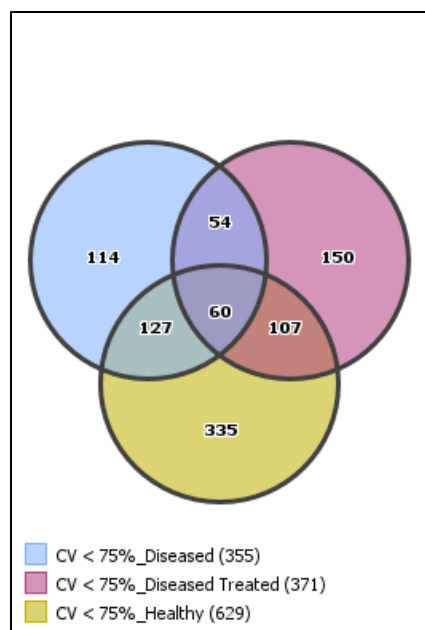


Figure S4. Representative Venn Diagram of those features with a %CV less than 75% (CV < 75%) for each sample group (diseased, diseased treated, and healthy). The total number of features passing this filter is shown in the parentheses after each group ID. Features passing the %CV filter in more than one group (overlapping regions) were selected for additional data processing. In this example, 348 features are found in the overlapping regions. Example shown was from the positive ionization mode profiling of brain homogenate samples using the microflow-based LC method.

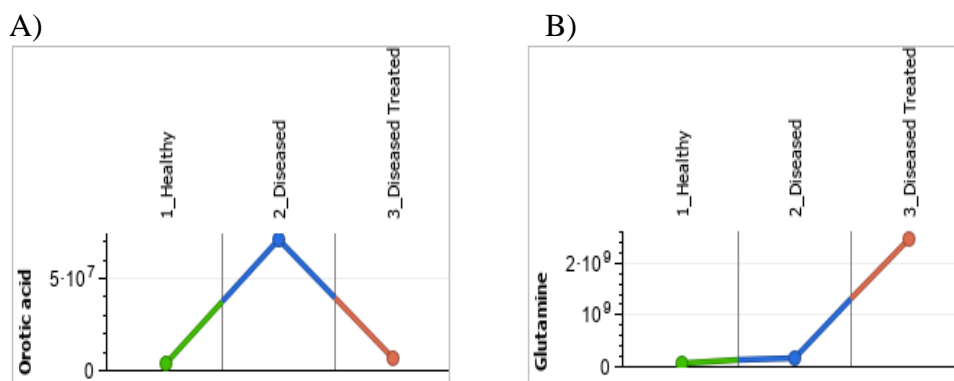
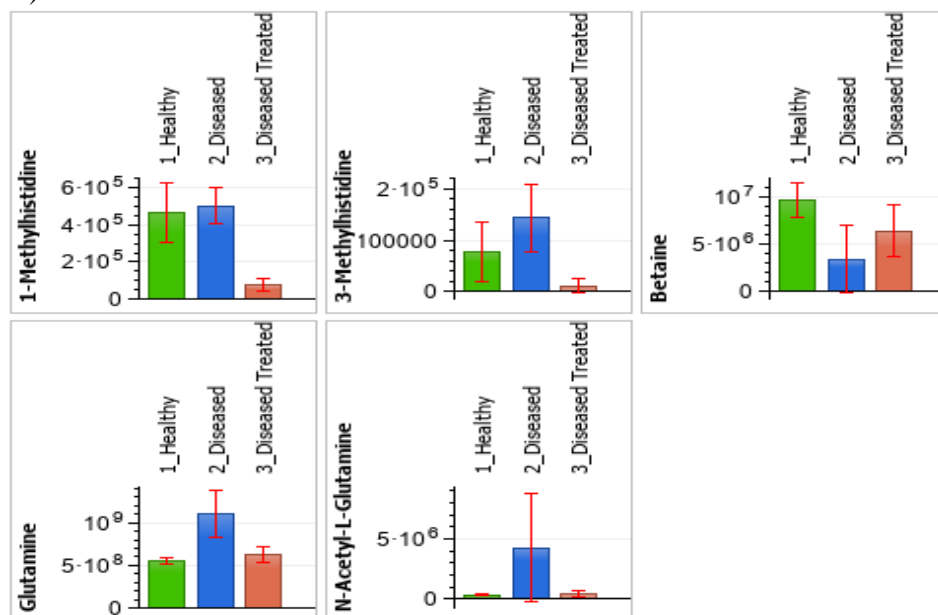


Figure S5. Representative trend plots of the normalized mean maximum intensity showing the desired trends for trend analysis filtering. A) Corrected by treatment in either the brain homogenate or urine samples and B) elevated with urinary excretion.

A)



B)

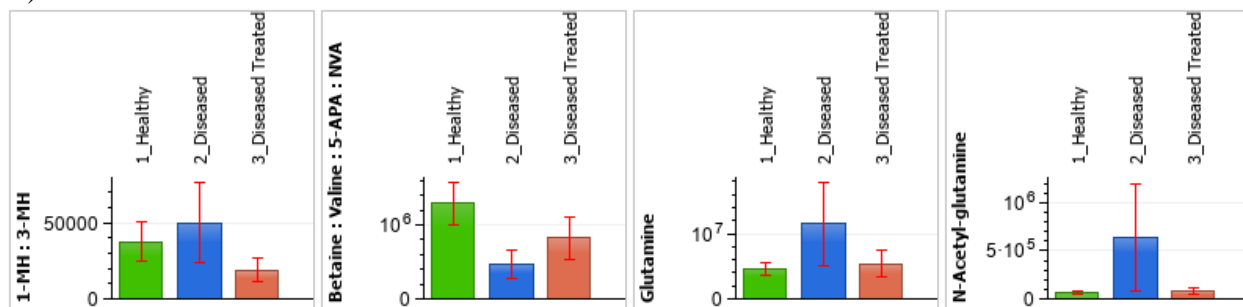


Figure S6. Graphs of the normalized mean maximum intensity for all identified metabolites present in mouse brain homogenate samples analyzed using the A) ion-pairing based method and the B) microflow-based LC method in the positive ionization mode. 1-MH: 1-Methylhistidine; 3-MH: 3-Methylhistidine; 5-APA: 5-Aminopentanoic acid; NVA: Norvaline

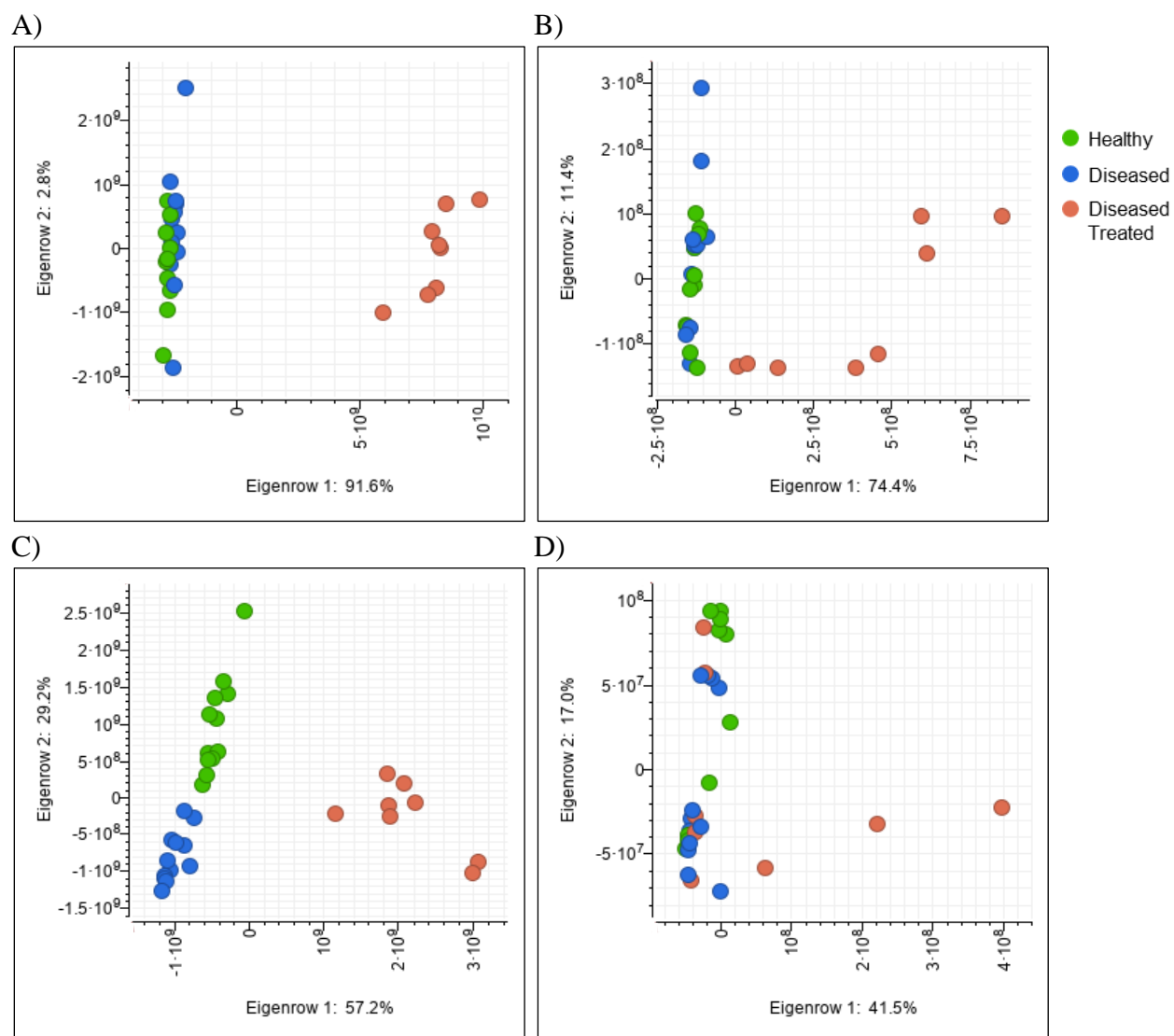


Figure S7. PCA plots of mouse urine samples. Shown are results from the positive ESI mode analysis using the A) ion-pairing-based LC method and B) microflow-based LC method; and the negative ESI mode analysis using the C) ion-pairing-based LC method and D) microflow-based LC method.

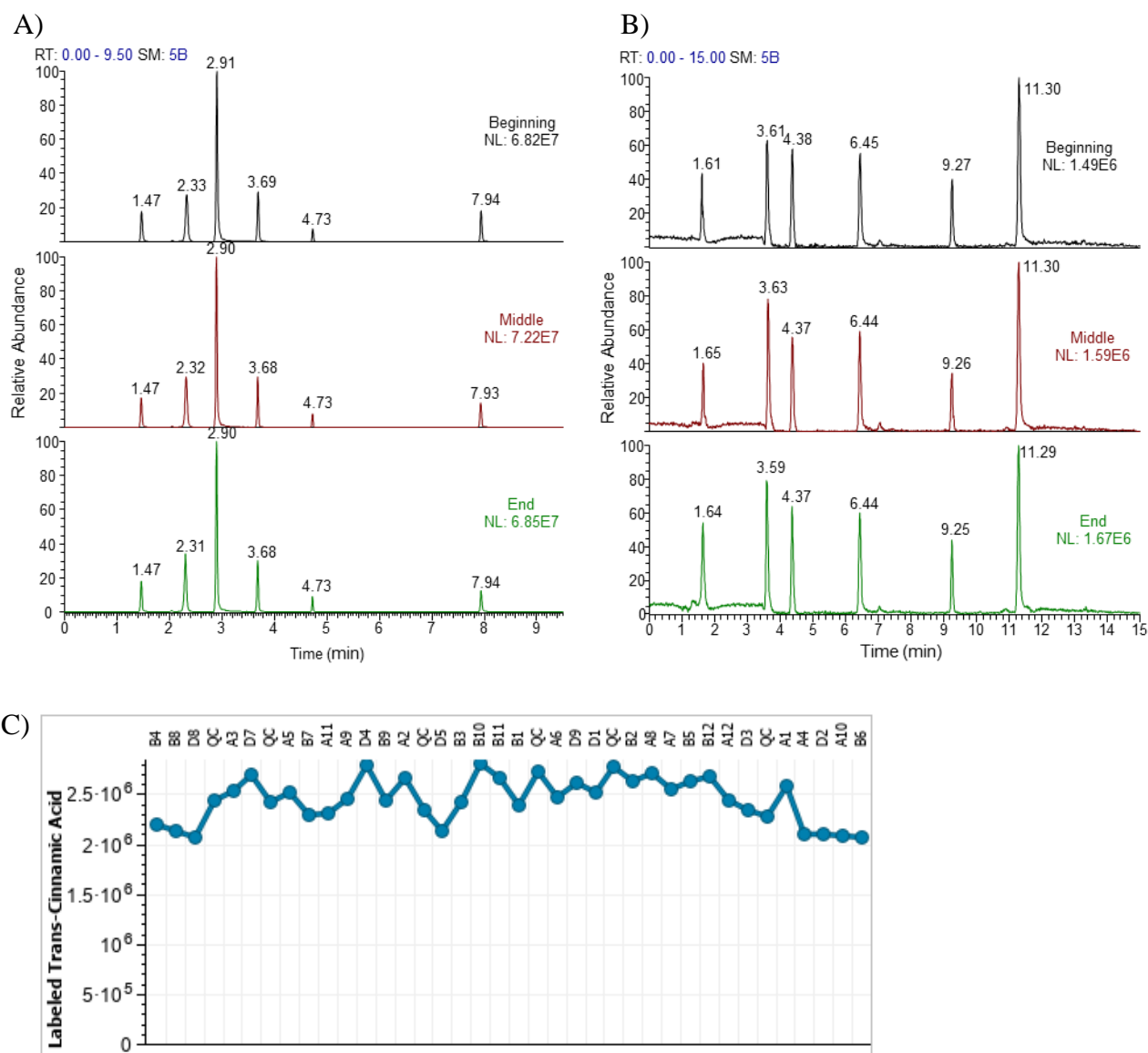


Figure S8. Representative results confirming the instrumental stability for the analysis of the urine samples analyzed using the microflow and analytical flow ion-pairing based methods in the positive ionization mode. A) Extracted ion chromatograms (5 ppm mass accuracy) of QC injections analyzed at the beginning, middle, and end of the ion-pairing method sequence. Analytes shown (from left to right): glutamine, threonine, cystine, lysine, 1-methylhistamine : 3-methylhistamine, tryptophan. B) Extracted ion chromatograms (5 ppm mass accuracy) of QC injections analyzed at the beginning, middle, and end of the reversed-phase microflow method sequence. Analytes shown (from left to right): lysine, histidine, glutamine, leucine : isoleucine, N-acetylalanine, tryptophan, isotopically labeled trans-cinnamic acid. C) The normalized maximum intensity of the isotopically labeled trans-cinnamic acid internal standard in all sample and QC injections analyzed using the microflow method. The percent relative standard deviation of the internal standards across all sample and QC injections was < 20% with both methods.

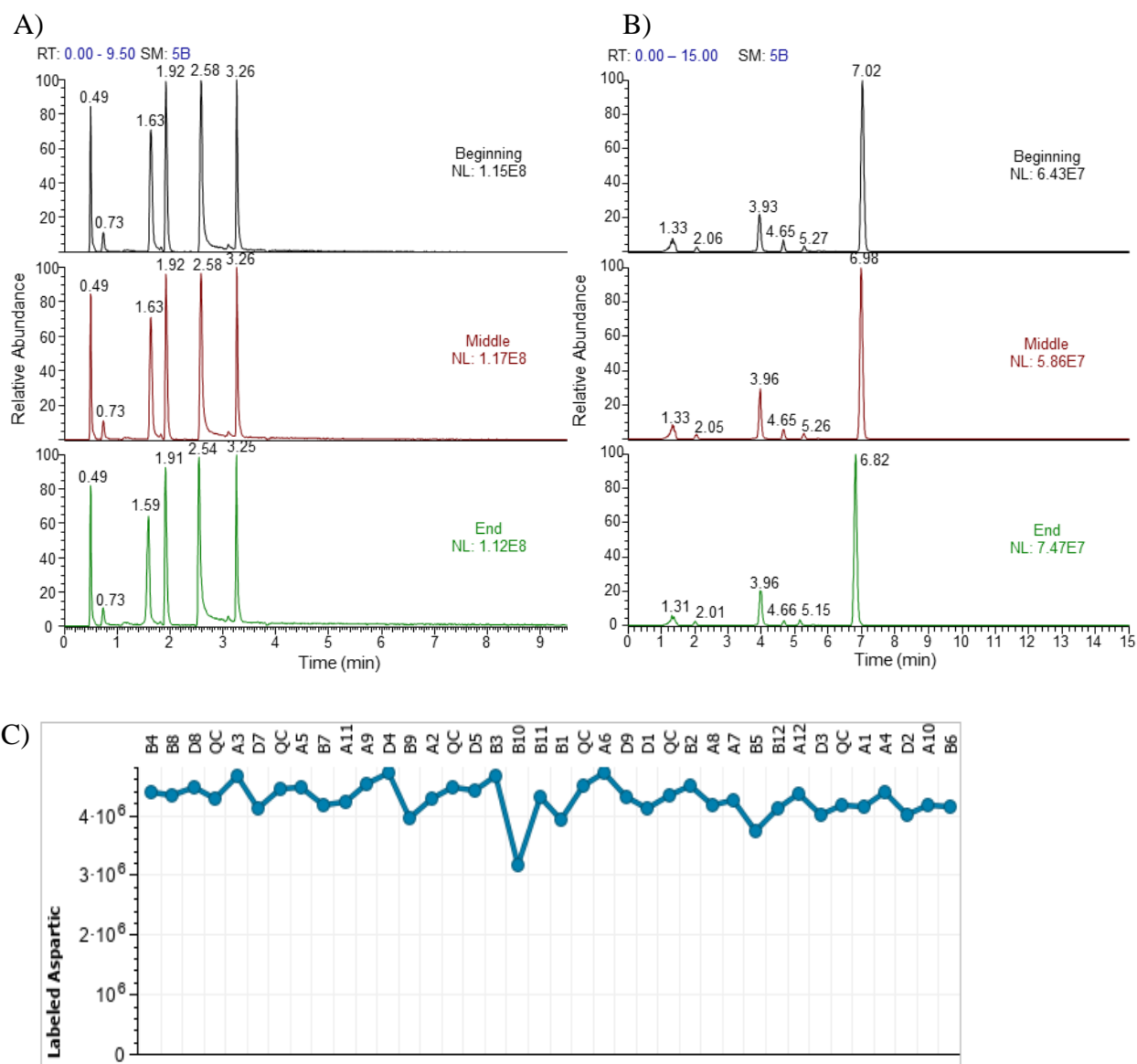


Figure S9. Representative results confirming the instrumental stability for the analysis of the urine samples analyzed using the microflow and analytical flow ion-pairing based methods in the negative ionization mode. A) Extracted ion chromatograms (5 ppm mass accuracy) of QC injections analyzed at the beginning, middle, and end of the ion-pairing method sequence. Analytes shown (from left to right): serine, pipecolic acid, tyrosine, N-acetyl-glutamine, phenylalanine, p-cresol glucuronide. B) Extracted ion chromatograms (5 ppm mass accuracy) of QC injections analyzed at the beginning, middle, and end of the reversed-phase microflow method sequence. Analytes shown (from left to right): homoserine : threonine, ureidopropionic acid, phenylalanine, tryptophan, N-acetylmethionine, p-cresol glucuronide. C) The normalized maximum intensity of the isotopically labeled aspartic acid internal standard in all sample and QC injections analyzed using the ion-pairing method. The percent relative standard deviation of the internal standards across all sample and QC injections was < 20% with both methods.

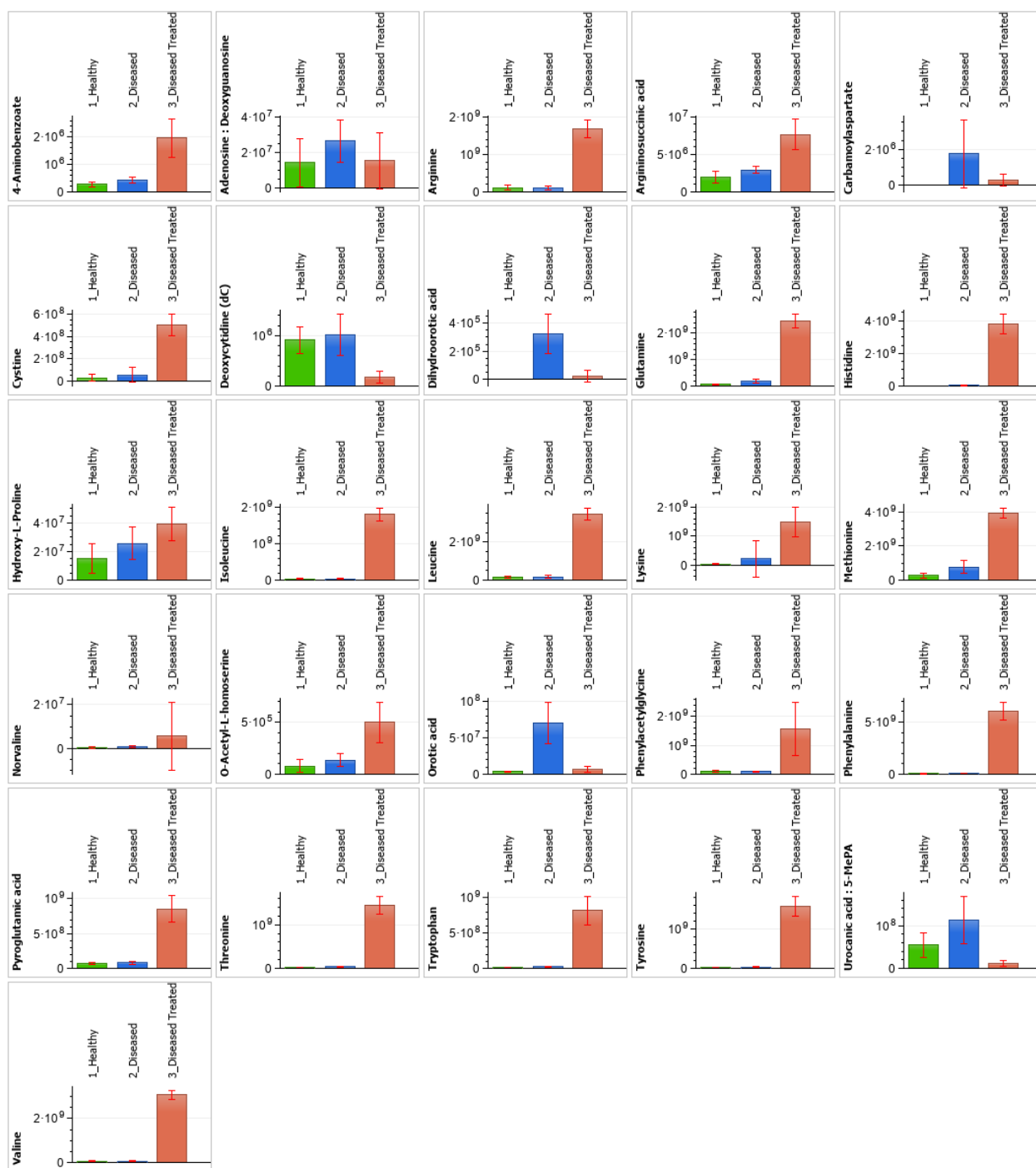


Figure S10. Graphs of the normalized mean maximum intensity for all identified metabolites present in mouse urine samples analyzed using the ion-pairing based method in the positive ionization mode. 5-MePA: 5-Methylpyrazine-2-carboxylic acid

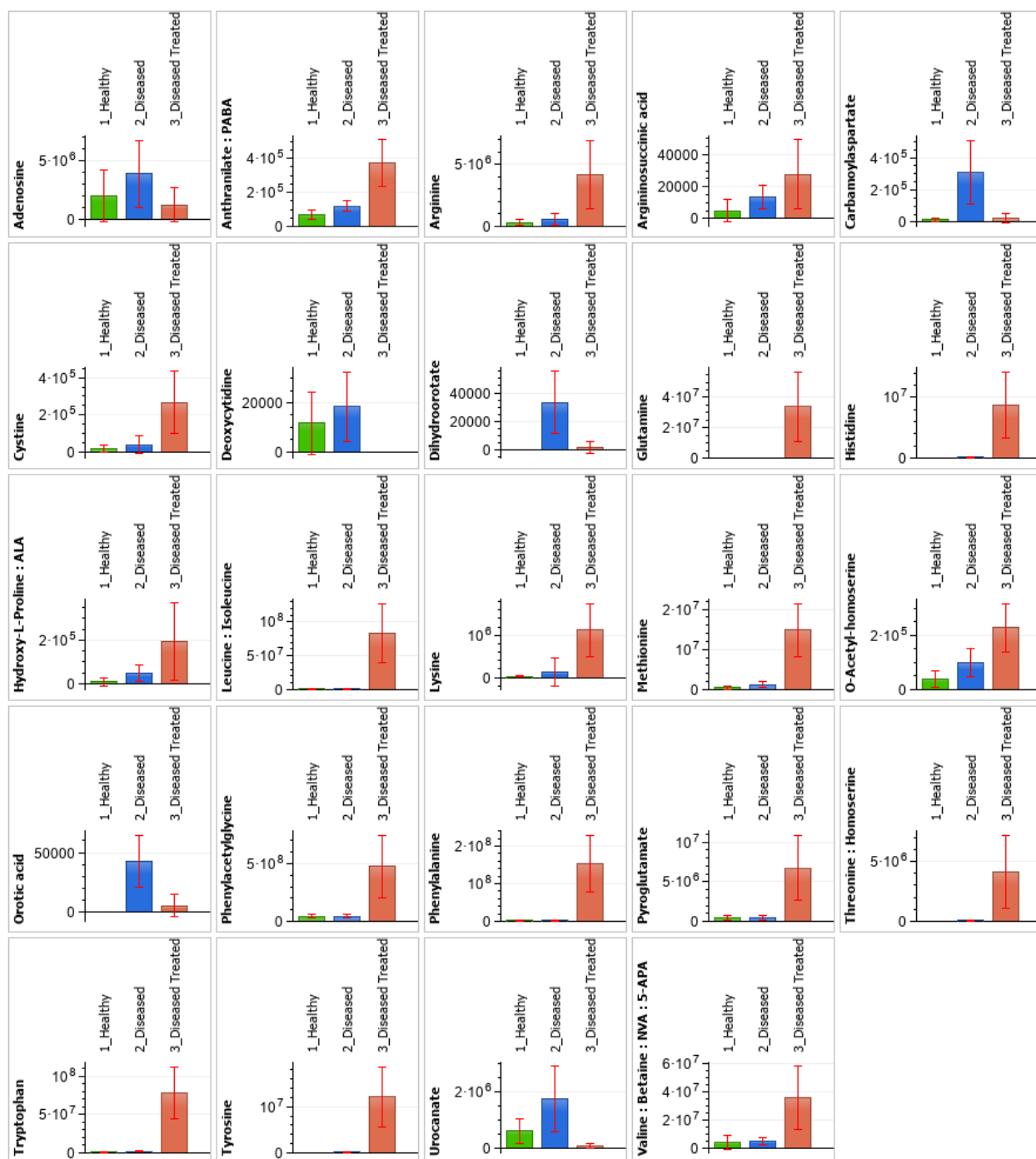


Figure S11. Graphs of the normalized mean maximum intensity for all identified metabolites present in mouse urine samples analyzed using the microflow method in the positive ionization mode. PABA: p-Aminobenzoic acid

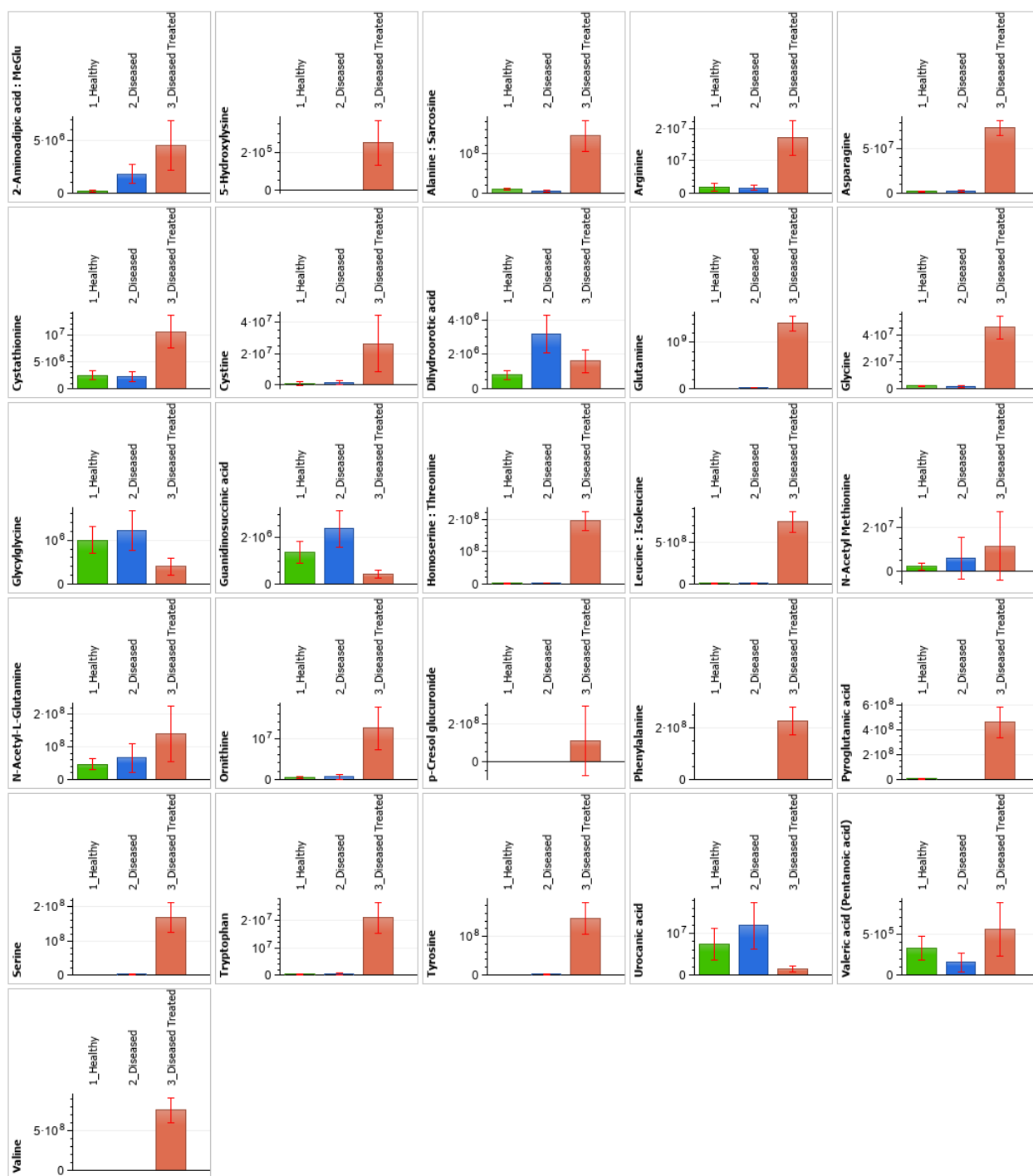


Figure S12. Graphs of the normalized mean maximum intensity for all identified metabolites present in mouse urine samples analyzed using the ion-pairing based method in the negative ionization mode. MeGlu: N-Methylglutamate

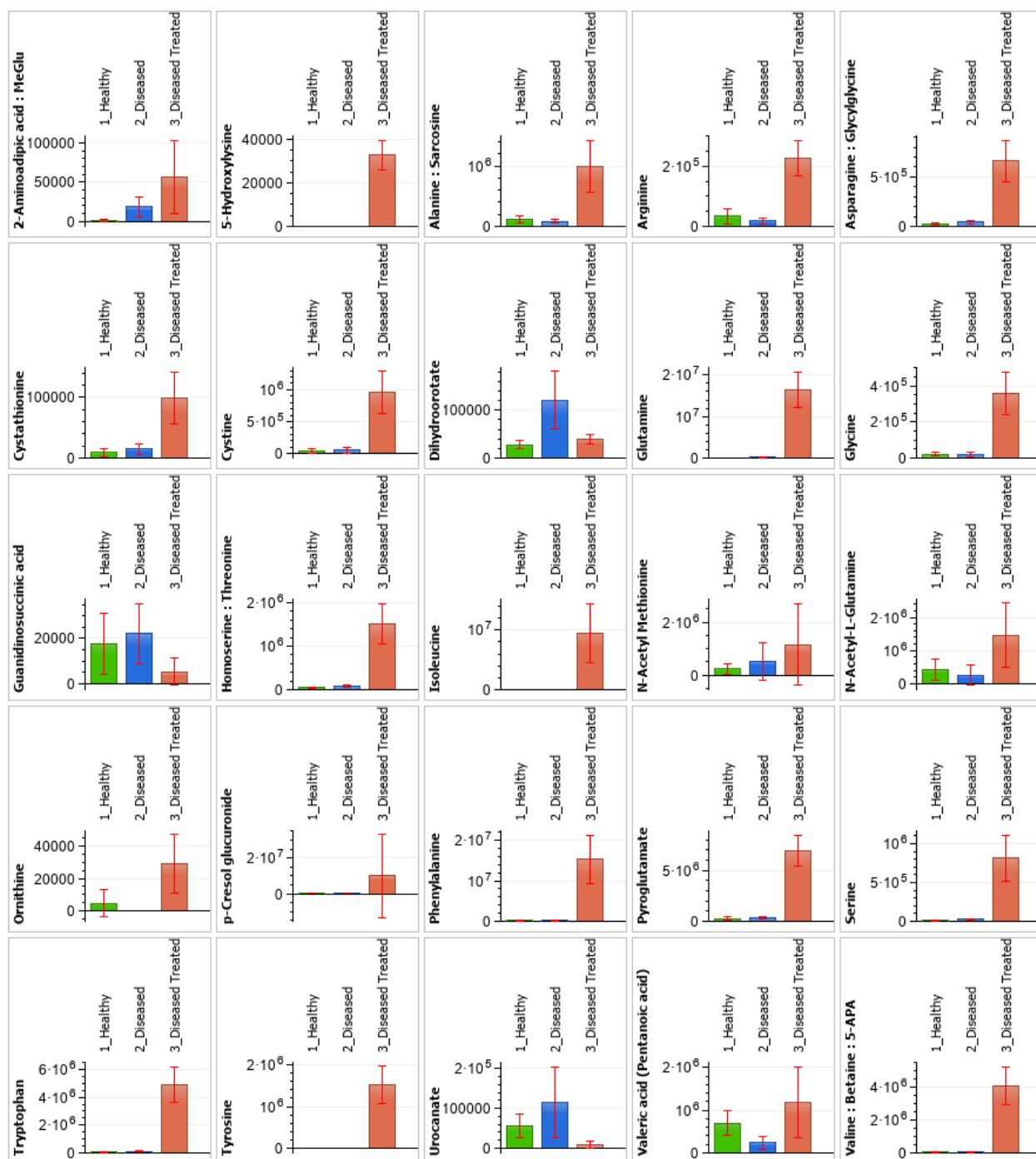


Figure S13. Graphs of the normalized mean maximum intensity for all identified metabolites present in mouse urine samples analyzed using the microflow method in the negative ionization mode. MeGlu: N-Methylglutamate; 5-APA: 5-Aminopentanoic acid

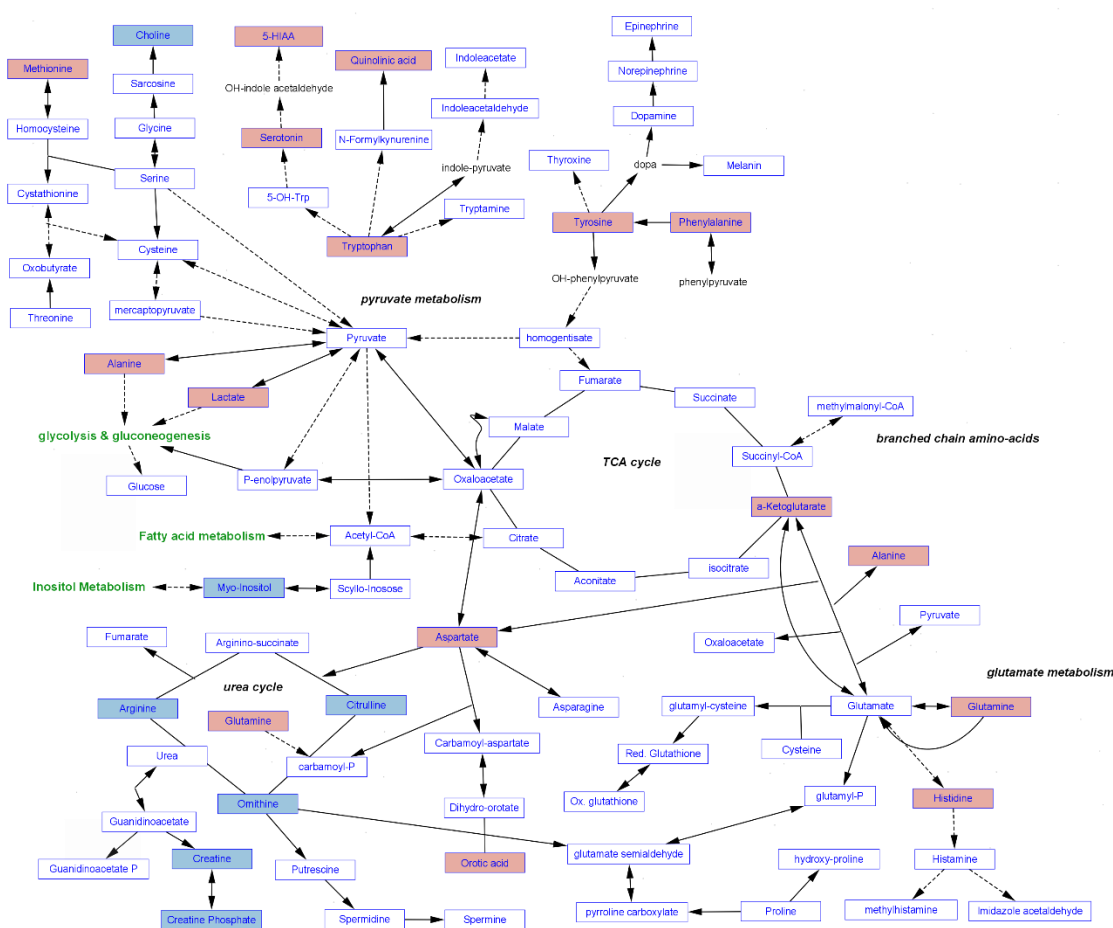


Figure S14. Metabolic pathway map highlighting known UCD biomarkers. Metabolites upregulated by the disease are shown in pink, while those metabolites which are downregulated by the disease are shown in blue. The pathway was generated using the WikiPathways app in Cytoscape v3.8.2.

Table S1. Percentage of features with a linear response detected in brain homogenate samples in the positive ionization mode with the microflow method during dilution factor optimization. The data is grouped by retention time window.

Retention Time Window	Neighboring Dilution Factors				Total Features
	30:60	60:90	90:120	120:150	
0 - 1	20	30	38	42	846
1 - 2	35	57	60	58	1979
2 - 3	21	27	29	28	739
3 - 4	24	34	36	33	1369
4 - 5	19	22	25	26	4161
5 - 6	20	27	27	25	4716
6 - 7	21	27	30	28	4999
7 - 8	21	28	27	26	4103
8 - 9	38	26	22	17	14007
9 - 10	34	26	22	21	12839
10 - 11	26	28	27	25	5316
11 - 12	31	34	41	39	2759
12 - 13	19	35	37	36	2186
13 - 14	20	29	27	34	1775
14 - 15	18	42	42	44	874
15 - 16	17	30	38	45	1086
16 - 17	6	21	18	39	101

Table S2. Percentage of features with a linear response detected in brain homogenate samples in the positive ionization mode with the microflow method during dilution factor optimization. The data is grouped by the m/z range.

m/z Window	Neighboring Dilution Factors				Total Features
	30:60	60:90	90:120	120:150	
0 - 100	19	25	28	28	6606
100 - 200	19	27	30	30	22716
200 - 300	20	43	47	46	5292
300 - 400	20	45	46	46	2877
400 - 500	18	59	63	64	453
500 - 600	38	50	58	51	175
600 - 700	46	41	35	30	351
700 - 800	42	25	18	13	7471
800 - 900	42	25	19	15	11825
900 - 1000	34	23	19	17	5910

Table S3. Number of brain homogenate samples per group analyzed using both the ion-pairing and microflow-based methods.

	Positive ESI Mode		Negative ESI Mode	
	Ion-Pairing	Microflow	Ion-Pairing	Microflow
Healthy	12	5	12	6
Diseased	12	12	12	11
Diseased Treated	9	9	9	6

Table S4. Number of urine samples per group analyzed using both the ion-pairing and microflow-based methods.

	Positive ESI Mode		Negative ESI Mode	
	Ion-Pairing	Microflow	Ion-Pairing	Microflow
Healthy	12	12	12	12
Diseased	12	12	12	12
Diseased Treated	8	8	8	8

Table S5. Summary of the metabolites identified in the brain homogenate samples analyzed using the ion-pairing and microflow based methods.

	Positive ESI Mode		Negative ESI Mode	
	Ion-Pairing	Microflow	Ion-Pairing	Microflow
Total Identified	21	10	8	2
Detected by Both Methods (#)	5		0	
Common Analyte (names)	1-Methyl-L-histidine; 3-Methyl-L-histidine; Betaine; Glutamine; N-Acetyl-glutamine		n/a	

Table S6. Data processing step where metabolites were filtered out of for mouse brain homogenate samples in the positive ionization mode.

Data Processing Step Metabolite Did Not Pass	Method Metabolite Did Not Pass Data Processing In			
	Ion-Pairing		Microflow	
	Number	Analyte Name	Number	Analyte Name
Analyte is not present in reference database			1	4-Methylene-L-glutamine
Standard was not detected*			1	Adenosine 5'-monophosphate/ Deoxyguanosine 5'-monophosphate
Peak not detected by GeneData**	1	N-Acetylleucine	8	α -ketoglutaric acid; Argininosuccinic acid; Cadaverine; Cystathionine; Hypotaurine; Kynurenine; Octopamine; Putrescine
p-value > 0.05	2	Adenosine; Glutaryl carnitine	5	Histidine; Hydroxy-L-proline; N-Methylaspartate; Pyroglutamate; Acetylspermidine
Effect size > 0.9	2	4-Guanidinobutanoate; Valine		
CV > 75%, or not present in 2+ groups			1	Diethanolamine
Incorrect trend				

* A retention time could not be obtained when the standard was tested

** Confirmed by manual XIC in the raw data

Table S7. Data processing step where metabolites were filtered out of for mouse brain homogenate samples in the negative ionization mode.

Data Processing Step Metabolite Did Not Pass	Method Metabolite Did Not Pass Data Processing In			
	Ion-Pairing		Microflow	
	Number	Analyte Name	Number	Analyte Name
Analyte is not present in reference database			1	6-Hydroxykynurenate
Standard was not detected*				
Peak not detected by GeneData**	1	Homovanillic acid	3	Methionine; Xanthurenic acid; N-Acetylglutamine;
p-value > 0.05			3	Glutamine; Lysine; Pyroglutamate
Effect size > 0.9	1	Allose/Fructose/ Galactose/Glucose/ Myo-inositol/Mannose/ Psicose/Sorbose/ Tagatose		
CV > 75%, or not present in 2+ groups			1	Histidine
Incorrect trend				

* A retention time could not be obtained when the standard was tested

** Confirmed by manual XIC in the raw data

Table S8. Summary of the metabolites identified in the urine samples analyzed using the ion-pairing and microflow-based methods.

	Positive ESI Mode		Negative ESI Mode	
	Ion-Pairing	Microflow	Ion-Pairing	Microflow
Total Identified	91	43	64	41
Common Analytes (#)	26		26	
Common Analyte (names)	4-Aminobenzoate; Adenosine/Deoxyguanosine (dG); Arginine; Argininosuccinic acid; Carbamoylaspartate; Cystine; Deoxycytidine; Dihydroorotic acid; Glutamine; Histidine; Hydroxy-proline; Isoleucine; Leucine; Lysine; Methionine; Norvaline; O-Acetyl-homoserine; Orotic acid; Phenylacetyl-glycine; Phenylalanine; Pyroglutamate; Threonine; Tryptophan; Tyrosine; Urocanic acid; Valine		2-Aminoadipic acid/ N-Methylglutamate; 5- Hydroxylysine; Alanine/Sarcosine; Arginine; Asparagine; Cystathionine; Cystine; Dihydroorotic acid; Glutamine; Glycine; Glycylglycine; Guanidinosuccinic acid; Homoserine/Threonine; Isoleucine; N-Acetyl-glutamine; N-Acetylmethionine; Ornithine; p-Cresol glucuronide (pCG); Phenylalanine; Pyroglutamate; Serine; Tryptophan; Tyrosine; Urocanate; Valeric acid; Valine	

Table S9. Data processing step where metabolites were filtered out of for mouse urine samples in the positive ionization mode.

Data Processing Step Metabolite Did Not Pass	Method Metabolite Did Not Pass Data Processing In			
	Ion-Pairing		Microflow	
	Number	Analyte Name	Number	Analyte Name
Analyte is not present in reference database			13	1-Methyl-6,7-dihydroxy-1,2,3,4-Tetrahydroisoquinoline; 4-Methylene-L-glutamine; 5-Acetamidopentanoate; 7-Methylguanosine; Homostachydrine; L- α -Aspartyl-L-hydroxyproline; Oxindole; Piperidine; Prolylleucine; Propanoyl phosphate; DL-Thiaproline; 5-Methylpyrazine-2-carboxylic acid; 6-Hydroxykynurenate
Standard was not detected*	1	Glutarate	11	3-Hydroxy-L-kynurenine; Benzylamine; Maleimide; N-Acetylglycine; Guanidinosuccinic acid; O-Phospho-L-serine; Picolinic acid; Quinolinic acid; 2-Hydroxyglutaric acid; 2-n-Tetrahydrothiophenecarboxylic acid; 5-Aminosalicylic acid;
Peak not detected by GeneData**	2	N-Formyl-L-methionine; O-Succinyl-homoserine	11	2,4-Dihydroxypteridine; 2-Aminoadipic acid; Cysteinesulfinic acid; Cadaverine; Cortisol; Cortisone; Dihydrofolate; Glucosamine; Glutathione; Homocystine; Phospho(enol)pyruvic acid
p-value > 0.05	8	3-Methylhistidine; 3-Methylhistamine; Histamine; N-Acetylalanine; 5-Aminolevulinate; N-Acetylneuraminic acid; Anthranilate; Betaine	16	2-Aminobutyric acid/3-Aminobutyric acid; 3,4-Dihydroxy-1-phenylalanine; 3-Methoxy-L-tyrosine; Alanine; Anserine; Biotin; Deoxyadenosine; Glycine; Homocysteine; Hypotaurine; Kynurenine; Pyridoxal; Homoarginine; Methionine Sulfoxide; N-Acetyl-L-valine; Saccharopine
Effect size > 0.9	6	1-Methylhistidine; 5-HIAA; 5-Hydroxytryptophan; Agmatine; Cysteine; Sarcosine	5	Adipic acid; Carnitine; Glutaryl carnitine; N,N,N-Trimethyl-L-lysine; Proline
CV > 75%, or not present in 2+ groups	1	Homoserine	7	Asparagine; Citrulline; Cystathionine; Glutamic acid; N-Methylaspartate; Ornithine; Serine
Incorrect trend			2	Homocitrulline; Xanthurenic acid

* A retention time could not be obtained when the standard was tested

** Confirmed by manual XIC in the raw data

Table S10. Data processing step where metabolites were filtered out of for mouse urine samples in the negative ionization mode.

Data Processing Step Metabolite Did Not Pass	Method Metabolite Did Not Pass Data Processing In			
	Ion-Pairing		Microflow	
	Number	Analyte Name	Number	Analyte Name
Analyte is not present in reference database			5	N-Methylhydantoin; Oxindole; p-Cresol sulfate (pCS); DL-Thiaproline; 6-Hydroxykynurenate
Standard was not detected*	3	Betaine; Homocysteine; Ureidopropionate	6	4-Methyl-2-oxo-pentanoic acid; Oxalic acid; 2-Hydroxyglutaric acid; Methionine Sulfoxide; N-acetyl-ornithine; Saccharopine
Peak not detected by GeneData**	6	Adenosine; Glucosamine/ Galactosamine/ Mannosamine; Kynurenine; Methionine; N-Methylaspartate; Pyridoxine	14	2-Oxoadipate; 3-Hydroxybutyrate; Citramalic acid; Fumaric acid; Maleic acid; Inosine 5'-monophosphate; Ketoglutaric acid; N-Acetyl-L-Phenylalanine; Ophthalmic acid; Quinolinic acid; S-Adenosylhomocysteine; Trigonelline; 3-Indoxylsulfate; Carbamoylaspartate
p-value > 0.05	4	5-HIAA; Fucose/Deoxyglucose /Rhamnose; Phosphoethanolamine; Taurine	6	4-Aminobutanoate/2-Aminobutyric acid/N,N-Dimethylglycine; Leucine; Malic acid; Orotic acid; Xanthurenic acid; Uridine
Effect size > 0.9	2	Aspartic acid; Pipecolate	3	Glutamic acid; Glycerol 3-phosphate; Phenylacetate
CV > 75%, or not present in 2+ groups			4	3,4-Dihydroxy-1-Phenylalanine; Citrulline; Histidine; Lysine
Incorrect trend				

* A retention time could not be obtained when the standard was tested

** Confirmed by manual XIC in the raw data